

Hyperlipidemia aggravates renal disease in B6.ROP Os/+ mice

ANJA S. MÜHLFELD,¹ MIN W. SPENCER,¹ KELLY L. HUDKINS, ELIZABETH KIRK, RENEE C. LEBOEUF, and CHARLES E. ALPERS

Department of Pathology, University of Washington, Seattle, Washington; Division of Nephrology and Immunology, University of Aachen, Aachen, Germany; and Department of Pathobiology, and Nutritional Sciences Interdisciplinary Program, University of Washington, Seattle, Washington

Hyperlipidemia aggravates renal disease in B6.ROP Os/+ mice.

Introduction. Reduction of renal mass is frequently associated with progressive loss of kidney function. We examined the effects of hyperlipidemia on renal pathology and mediators of tissue damage in B6.ROP Os/+ mice, a model of reduced renal mass.

Methods. C57BL/6 control mice and B6.ROP Os/+ mice were fed normal rodent chow or a high fat, high cholesterol (HFHC) diet for 12 weeks. Kidney function and renal pathology were assessed.

Results. Hyperlipidemia led to a decline in kidney function in C57BL/6 mice. Renal pathology was characterized by an increase in glomerular matrix and cellularity, glomerular and tubulointerstitial macrophage influx, and increased tubular epithelial cell turnover. Chow-fed B6.ROP Os/+ animals demonstrated glomerular hypertrophy with an increase in mesangial matrix and cellularity that was characterized by macrophage influx and increased proliferation. The tubulointerstitium showed increased macrophages as well as tubular atrophy and dilation. Renal pathology was accompanied by an increase in blood urea nitrogen (BUN) and proteinuria. Hyperlipidemia in B6.ROP Os/+ mice resulted in increased plasma BUN compared to chow-fed B6.ROP Os/+ animals and aggravated renal pathology by further increasing glomerular matrix and glomerular hypercellularity. Glomerular hypercellularity was associated with increased expression of platelet-derived growth factor-B (PDGF B) and its receptor β . Glomerular transforming growth factor- β (TGF- β) mRNA expression was increased in B6.ROP Os/+ mice, hyperlipidemic C57BL/6 mice and hyperlipidemic B6.ROP Os/+ animals compared to controls and correlated with the amount of mesangial matrix.

Conclusion. This study demonstrates that hyperlipidemia worsens renal pathology in B6.ROP Os/+ mice with a decline in renal function mediated at least in part through increased renal expression of the cytokines PDGF B and TGF- β .

The reduction of glomerular filtration rate (GFR) below 50% of normal has been associated with a progressive loss of kidney function, even after the original disease becomes inactive [1, 2]. There have been reports that up to 30% of patients with greater than 50% reduction of total renal mass develop systemic hypertension and 70% develop significant proteinuria, in some cases leading to end-stage renal disease (ESRD) [3, 4]. However, since most patients after unilateral nephrectomy are able to maintain normal kidney function it is clear that additional nonimmune mechanisms are important in the pathogenesis of chronic renal injury. Here, we assess the effects of two physiologic processes, reduced renal mass and hyperlipidemia, that have both been strongly implicated as key mediators of progressive renal injury. To study the role of reduced renal mass we utilized the ROP Os/+ mouse strain, which carries a radiation-induced mutation of the Os gene located on chromosome 8 [5, 6]. A homozygous mutation in this locus is associated with early postimplantation lethality, whereas heterozygous mice develop oligosyndactyly and 38% reduction in renal mass [7]. Mice develop an approximately 50% decrease in nephron number with a compensatory increase in glomerular volume and tubular hypertrophy [7]. This increase in glomerular volume is due to a significant expansion of the mesangial matrix area with accumulation of collagen IV and tenascin as well as an increase in glomerular cell number and concomitantly increased thymidine labeling index [8]. The Os mutation was originally described in ROP mice, which were shown to be a sclerosis prone strain [9, 10]. The B6.ROP Os/+ strain has all the biologic features of the Os mutation but is on a C57BL/6 genetic background, and not on a ROP background, despite the similarities in nomenclature. This strain is neutral with respect to susceptibility to glomerulosclerosis, and is more resistant to sclerosis than the ROP strain originally used for studies of the renal effects of the Os mutation.

Abnormal lipid metabolism frequently accompanies renal disease and is thought to be involved in the pathogenesis of renal injury. Clinical observations have

¹Min W. Spencer and Anja S. Mühlfeld contributed equally to this work.

Key words: hyperlipidemia, extracellular matrix, ROP Os/+.

Received for publication August 5, 2003

and in revised form March 4, 2004

Accepted for publication April 16, 2004

© 2004 by the International Society of Nephrology

suggested a role of hyperlipidemia as a modulator of progression of primary kidney diseases. Nondiabetic patients with proteinuria and elevation in serum cholesterol and triglycerides had a nearly twofold increase in the rate of loss of renal function compared to normolipidemic patients [11, 12] and treatment with lipid-lowering agents has been demonstrated to reduce levels of circulating cholesterol and to stabilize or improve renal function [13–15]. However, the relationship between hyperlipidemia and renal injury remains incompletely understood. The aim of this study was to gain further insight into the effects of hyperlipidemia on renal pathology and kidney function in a model of reduced renal mass, the B6.ROP Os/+ mouse.

METHODS

Animal study and experimental design

Female C57BL/6 and male B6.ROP Os/+ mice were obtained from the Jackson Laboratory (Bar Harbor, ME, USA). C57BL/6 females were bred with the B6.ROP Os/+ males to generate mice heterozygous for the Os gene. Female C57BL/6 control mice and B6.ROP Os/+ were fed either a rodent chow diet ($N = 5$ and $N = 6$, respectively), or a high fat, high cholesterol (HFHC) diet ($N = 5$, and $N = 8$, respectively) as described below. Mice were maintained in a temperature-controlled room (22°C) with a 12-hour light/dark cycle and given free access to food and water. Food was removed from the mice 4 hours prior to the collection of blood from the retroorbital sinus into tubes containing anticoagulant [1 mmol/L ethylenediaminetetraacetic acid (EDTA)]. Plasma was stored at -70°C until analysis. Mice were killed by cervical dislocation and tissues were snap frozen in liquid nitrogen and stored at -70°C.

Diets and feeding

Two diets were used in this study. The first was pelleted rodent chow (Wayne Rodent BLOX 8604), which served as a reference diet and contained by weight approximately 4% fat, 24% protein, and 4.5% crude fiber (manufacturer's estimates). All mice were fed the rodent chow diet until 20 weeks of age when the test diet was initiated in the experimental group. The test diet was a HFHC diet that contained 15% fat, 1.25% cholesterol, and 0.5% sodium cholate (TD 92001) (Harlan Teklad, Madison WI, USA). Mice were fed the HFHC diet for 12 weeks.

Analytical procedures

Total plasma cholesterol was assessed colorimetrically using a kit from Diagnostic Chemicals Limited (Diagnostic Chemicals Limited, Oxford, CT, USA) with cholesterol standards (Preciset #12552) (Boehringer Mannheim, Indianapolis, IN, USA). Plasma triglyceride

levels were determined after the removal of free glycerol using a colorimetric kit (Diagnostic kit # 450032) (Boehringer Mannheim). Plasma blood urea nitrogen (BUN) levels were measured using a colorimetric assay from Sigma (Diagnostic kit #535-A) (Sigma Chemical Co., St. Louis, MO, USA). Urinary protein excretion was assessed with urine test strips (Uristix) (Bayer, Elkhart, IN, USA) in a semiquantitative fashion. Glucose and insulin levels were measured at the Northwest Lipid Research Laboratories, University of Washington.

Tissue preparation and histologic staining

At the end of the study mice were sacrificed by cervical dislocation and whole animals were perfused with 10 mL of antioxidant buffer [100 µmol/L diethylenetriamine pentaacetic acid (DTPA), 100 µmol/L, butylated hydroxytoluene (BHT), and 0.1% ethanol in phosphate-buffered saline (PBS), pH 7.4] via the left ventricle. Kidneys were removed and fixed in 10% neutral buffered formalin or methyl Carnoy's solution (60% methanol, 30% chloroform, and 10% acetic acid) for histologic examination. Small portions of kidney tissue were fixed in half strength Karnovsky's solution for electron microscopy (1% paraformaldehyde and 1.25% glutaraldehyde in 0.1 mol/L Na cacodylate buffer, pH 7.0). Tissues were processed and embedded in paraffin using standard protocols and cut into 2 µm sections for periodic acid-methenamine silver stain (PAM) or in 4 µm sections for hematoxylin and eosin staining, immunohistochemistry or terminal deoxy transferase uridine triphosphate nick end labeling (TUNEL) staining.

Immunohistochemistry and TUNEL staining

Tissue sections were deparaffinized in xylene and rehydrated in graded ethanol to use for immunohistochemistry. Where necessary, antigen retrieval was performed by heating tissue sections in Antigen Unmasking Solution (Vector Laboratories, Burlingame, CA, USA). Endogenous peroxidases were blocked by immersing the tissue in 3% hydrogen peroxide and endogenous biotin was blocked using the Avidin/Biotin blocking kit (Vector Laboratories). Primary antibodies were diluted in 1% bovine serum albumin (BSA) (Sigma Chemical Co.) in PBS and sections were incubated for 1 hour at room temperature. After repeated washing steps slides were incubated with the appropriate biotinylated secondary antibody for 30 minutes. Signal amplification was performed with the Vector ABC-Elite Reagent and 3, 3'-diaminobenzidine (DAB) (Sigma Chemical Co.) with nickel enhancement was used a chromogen resulting in a black color product. Tissue sections were counterstained with periodic acid-Schiff (PAS)/methyl green, dehydrated and coverslipped.

Macrophages were detected with a rat anti-mouse Mac-2 antibody from Cederlane (Cederlane, Ontario,

Canada) as described previously [16]. Mesangial cell activation and smooth muscle-like transformation was assessed with a mouse monoclonal IgG_{2a} antibody against α -smooth muscle actin (α -SMA) (clone 1A4) (Dako, Carpinteria, CA, USA), previously described in [17]. An antibody against human proliferating cell nuclear antigen (PCNA) (Oncogene Research Products, Cambridge, MA, USA) was used to show cellular proliferation (previously described in [18]). Glomerular apolipoprotein B deposition was stained with a rabbit polyclonal antibody generously provided by J. Born. Appropriate secondary antibodies were all from Vector Laboratories except for antimouse IgG_{2a}, which was purchased from Pharmingen (San Diego, CA, USA).

TUNEL staining was performed using the TdT-FragEL DNA fragmentation detection kit (Oncogene Research Products) according to the manufacturer's instructions and previously described in detail [19]. In brief, tissue sections were deparaffinized, rehydrated, and permeabilized in 20 μ g/mL proteinase K in 10 mmol/L Tris. Endogenous peroxidases were blocked in 3% hydrogen peroxide in methanol. After that slides were labeled with TdT labeling reaction mix and incubated for 1.5 hours at 37°C. The resulting signal was amplified with the ABC-Elite reagent (Vector Laboratories) and visualized with DAB and nickel enhancement. Finally, the slides were counterstained with PAS and methyl green, dehydrated, and coverslipped.

In situ hybridization

In situ hybridization was performed on formalin fixed tissue after washing in 0.5 \times standard saline citrate (SSC) (1 \times SSC = 150 mmol/L NaCl and 15 mmol/L Na citrate, pH 7.0) and digestion with 25 μ g/mL proteinase K (Sigma Chemical Co.) for 30 minutes at 37°C. Several washes with 0.5 \times SSC are followed by a 2-hour incubation with prehybridization buffer [0.3 mol/L NaCl, 20 mmol/L Tris, pH 8.0, 5 mmol/L EDTA, 1 \times Denhardt's solution, 10% dextran sulfate, and 10 mmol/L dithiothreitol (DTT)]. The hybridization process was started by adding 500,000 cpm ³⁵S-labeled probe in prehybridization buffer to the slides and allowed to proceed overnight at 50°C. After hybridization the slides were washed in 2 \times SSC and treated with RNase A (20 μ g/mL). Rinsing in 2 \times SSC was followed by three high-stringency washing steps in 0.1 \times SSC + 0.1% Tween 20 (Sigma Chemical Co.) at 50°C and several 2 \times SSC washes. The tissue was then dehydrated in graded ethanol, air-dried, and dipped in NTB2 nuclear emulsion (Kodak, Rochester, NY, USA). Slides were exposed in the dark for 2 to 5 weeks at 4°C. After developing the sections were counterstained with hematoxylin and eosin.

Probes used for in situ hybridization were transforming growth factor- β (TGF- β 1), platelet-derived growth factor-B (PDGF-B), PDGF receptor β , and monocyte

chemoattractant protein-1 (MCP-1) and have been described in detail [20].

Electron microscopy

Randomly selected cases of each experimental group were utilized for electron microscopy and processed as described previously in detail [21]. Grids were scanned using a Philips 410 electron microscope (Philips, Eindhoven, The Netherlands).

Quantitative analysis and statistics

Morphometric analysis was performed by using the Image Pro Plus software (Media Cybernetics, Silver Spring, MD, USA). Fifteen random glomerular cross-sections per experimental animal were photographed by a blinded examiner using a digital camera (Olympus DP11) (Olympus America, Melville, NY, USA). Hematoxylin and eosin-stained sections were used for the assessment of glomerular cellularity while the amount of extracellular matrix was evaluated using PAM silver stains and immunohistochemistry for collagen IV. The number of macrophages and proliferating cells was counted in at least 20 random glomerular cross-sections or high power fields. Glomerular α -SMA expression in mesangial areas was assessed semiquantitatively on a scale from 0 (negative) to 4 (strong global expression) as previously described [22]. Intraglomerular expression of mRNA for different probes was scored using a similar semiquantitative system in which 0 corresponded to no expression, 1 to only a few positive cells, 2 to several positive cells, and 3 to many positive cells in a diffuse distribution.

Values are expressed as mean \pm SEM. Statistical differences were calculated using the SPSS software (SPSS Inc., Chicago, IL, USA). Means between groups were compared using analysis of variance (ANOVA) with Tukey's post hoc test. A *P* value of *P* < 0.05 was considered statistically significant. Association between PDGF-B and glomerular cellularity as well as TGF- β and glomerular matrix and collagen IV expression was calculated using the nonparametric Spearman rank correlation coefficient.

RESULTS

Hyperlipidemia reduced kidney function and induced renal pathology in C57BL/6 mice

Feeding of a HFHC diet to C57BL/6 mice led to a significant increase in plasma cholesterol from 63 \pm 4 mg/dL in control animals to 249 \pm 27 mg/dL in the HFHC diet (*P* < 0.01) (Table 1) while plasma triglycerides levels decreased from 36 \pm 5 mg/dL for controls to 9 \pm 1 mg/dL in animals on the HFHC diet. These changes in lipid metabolism were accompanied by a significant increase in plasma BUN in the hyperlipidemic group (26 \pm 2 mg/dL in controls vs. 41 \pm 4 mg/dL in hyperlipidemic animals) (*P* < 0.05) (Table 1) and a significant increase

Table 1. Laboratory data

	C57BL/6, chow	C57BL/6, high fat diet	B6.ROP Os/+, chow	B6.ROP Os/+, high fat diet
Cholesterol mg/dL	65 ± 4	249 ± 27 ^b	71 ± 3	361 ± 41 ^{b,f}
Triglycerides mg/dL	35 ± 5	9 ± 1 ^b	34 ± 4	18 ± 3 ^{b,e}
BUN mg/dL	26 ± 2	41 ± 4 ^a	45 ± 4 ^b	62 ± 2 ^{c,d,g}
Proteinuria ^h	0.4 ± 0.2	1.4 ± 0.2 ^a	1.5 ± 0.2 ^b	1.9 ± 0.1 ^c
Glucose mg/dL	143 ± 6 ^d	127 ± 23 ^d	200 ± 10 ^a	108 ± 5 ^d
Insulin ng/mL	0.4	0.2 ± 0.1	0.4 ± 0.1	0.2 ± 0.0

BUN is blood urea nitrogen.

Lipid metabolism and kidney function in chow fed C57BL/6 wild-type and B6.ROP Os/+ mice and C57BL/6 and B6.ROP Os/+ animals on a high fat diet. Data expressed as mean ± SEM. Statistical significances compared to wild-type controls (^a $P < 0.05$, ^b $P < 0.01$, ^c $P < 0.001$) or compared to chow-fed B6.ROP Os/+ animals (^d $P < 0.05$, ^e $P < 0.01$, ^f $P < 0.001$).

^gMarks statistically significant differences at a level of $P < 0.01$ between hyperlipidemic C57BL/6 mice and hyperlipidemic B6.ROP Os/+ animals.

^hProteinuria assessed by dipstick: 1 = 30 mg/dL, 2 = 100 mg/dL.

Table 2. Morphometric data

	C57BL/6, chow	C57BL/6+, high fat diet	B6.ROP Os/+, chow	B6.ROP Os/+, high fat diet
Glomerular size μm^2	3679 ± 134	4394 ± 140	6045 ± 383 ^c	5414 ± 159 ^{c,g}
Extracellular matrix/gcs μm^2	179 ± 15	325 ± 30 ^b	355 ± 29 ^b	396 ± 24 ^c
Extracellular matrix/area % glomerular area	4.5 ± 0.4	7.7 ± 0.3 ^c	5.8 ± 0.3 ^a	7.1 ± 0.3 ^{c,d}
Collagen IV/gcs μm^2	237 ± 24	399 ± 29 ^b	563 ± 28 ^c	673 ± 25 ^{c,e,h}
Collagen IV/area % glomerular area	6.1 ± 0.3	8.1 ± 0.4	8.7 ± 0.2 ^c	12.2 ± 0.4 ^{c,d}
Cellularity cells/gcs	43 ± 2	58 ± 1 ^b	64 ± 4 ^c	66 ± 2 ^c
Cellularity/area % glomerular area	12 ± 0.2	14 ± 0.2 ^b	11 ± 0.5 ^a	12 ± 0.2 ^{e,g}
Proliferation PCNA-positive cell/gcs	0 ± 0	0.2 ± 0.08	0.3 ± 0.11 ^a	0.1 ± 0.04
Proliferation PCNA-positive cell/hpf	1.2 ± 0.3	7.4 ± 0.8 ^b	1.8 ± 0.2	9.8 ± 1.4 ^{c,f}
Glomerular apoptosis	0.000 ± 0.000	0.020 ± 0.010	0.013 ± 0.006	0.006 ± 0.004
TUNEL-positive cells/gcs		NS	NS	NS
Tubulointerstitial apoptosis	0.0 ± 0.0	0.8 ± 0.4	0.5 ± 0.2	0.6 ± 0.2
TUNEL-positive cells/20 hpf		NS	NS	NS
Macrophage infiltration Mac-2-positive cells/gcs	1.2 ± 0.2	0.9 ± 0.2	3.6 ± 0.7 ^b	2.0 ± 0.1 ^d
Macrophage infiltration Mac-2-positive cells/hpf	0.2 ± 0.0	3.6 ± 0.4 ^b	2.5 ± 0.6 ^a	3.7 ± 0.5 ^c
α -smooth muscle actin expression	0.0 ± 0.01	0.2 ± 0.04 ^a	0.6 ± 0.03 ^c	0.3 ± 0.02 ^{c,f,h}

Abbreviations are: gcs, glomerular cross-section; hpf, high power field; PCNA, proliferating cell nuclear antigen; TUNEL, terminal deoxy transferase uridine triphosphate nick end labeling.

Morphometric analysis of kidney sections from chow-fed wild-type and B6.ROP Os/+ mice and C57BL/6 and B6.ROP Os/+ animals on a high fat diet. Data expressed as mean ± SEM. Statistical significances compared to wild-type controls (^a $P < 0.05$, ^b $P < 0.01$, ^c $P < 0.001$) or compared to chow fed B6.ROP Os/+ animals (^d $P < 0.05$, ^e $P < 0.01$, ^f $P < 0.001$). Statistically significant differences between both hyperlipidemic groups are expressed as ^g $P < 0.05$ and ^h $P < 0.01$.

in urinary protein excretion (0.4 ± 0.2 units in C57BL/6 mice vs. 1.4 ± 0.2 units in mice fed the HFHC diet) ($P < 0.05$) (Table 1).

This decline in kidney function by hyperlipidemia correlated with the induction of renal pathology in C57BL/6 mice. Hyperlipidemic mice showed modest amounts of glomerular staining for apolipoprotein B, which was absent in normolipidemic mice (Fig. 5). Glomerular lesions were represented by an increase in mesangial α -SMA expression (score of 0.0 ± 0.0 in wild-type mice vs. 0.2 ± 0.0 in animals fed the HFHC diet) ($P < 0.05$) (Table 2) (Fig. 3). This indication of mesangial cell activation corresponded to a twofold increase in mesangial matrix ($P < 0.01$) and glomerular collagen IV ($P < 0.001$) in hyperlipidemic mice compared to normal control mice (Table 2) (Fig. 1). Glomeruli of hyperlipidemic C57BL/6 mice also demonstrated modest hypercellularity with an increase in cell number from 43 ± 2 cells/glomerular cross-section in control mice to 58 ± 1 cells/glomerular cross-section in animals fed the HFHC diet ($P < 0.01$) (Table 2) (Fig. 1). Proliferation and apoptotic cell death, assessed by PCNA

and TUNEL staining, were not different between mice on normal chow and animals fed a HFHC diet. Glomerular macrophage content was only slightly elevated in hyperlipidemic mice compared to controls but glomerular macrophages had frequently foam cell appearance (Table 2) (Fig. 2).

In addition to the glomerular changes induced by hyperlipidemia, mice on the HFHC diet also demonstrated tubulointerstitial pathology. Hyperlipidemic mice showed occasional staining for apolipoprotein B in infiltrating cells in the tubulointerstitium, morphologically most likely representing macrophages (Fig. 5). They had a large influx of macrophages into the tubulointerstitium (3.6 ± 0.4 mac-2-positive cells/high power field vs. 0.2 ± 0.0 cells/high power field in control mice) ($P < 0.01$) (Table 2) (Fig. 4). Hyperlipidemic mice showed signs of fatty degeneration of the tubular epithelium and cellular proliferation was significantly increased in the tubular epithelium (1.2 ± 0.3 PCNA positive cells/high power field in control mice vs. 7.4 ± 0.8 cells/high power field in mice fed the HFHC diet) ($P < 0.01$) (Table 2).

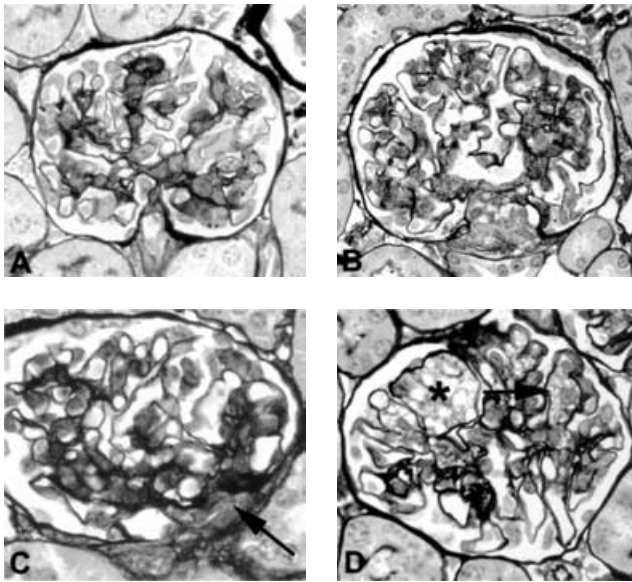


Fig. 1. Glomerular architecture in control and hyperlipidemic mice. (A) Normal glomerular architecture in a chow fed C57BL/6 wild-type mouse. (B) C57BL/6 animal, high fat, high cholesterol diet. The glomerulus shows a segmental increase in extracellular matrix. (C) Glomerulus from a chow-fed B6.ROP Os/+ mouse with segment expansion of the mesangial matrix and adhesion of the glomerular tuft to Bowman's capsule (arrow). (D) B6.ROP Os/+ animal fed the high fat, high cholesterol diet. The glomerulus demonstrates an area of mesangiolysis (*) and a prominent foam cell (arrow).

B6.ROP Os/+ mice showed glomerular hypertrophy and mesangial accumulation of extracellular matrix

B6.ROP Os/+ mice demonstrated a significant decline in renal function compared to C57BL/6 control mice. Plasma BUN levels were elevated to 45 ± 4 mg/dL compared to 26 ± 2 mg/dL in controls ($P < 0.01$) (Table 1) and proteinuria increased from $0.4 \pm 0.2 \times$ in C57BL/6 animals to $1.5 \pm 0.2 \times$ in mice with the Os gene ($P < 0.01$) (Table 1). Plasma cholesterol and triglycerides levels remained unchanged.

Renal pathology was remarkable for glomerular hypertrophy, demonstrated by an increase in glomerular size ($3679 \pm 134 \mu\text{m}^2$ in controls vs. $6045 \pm 383 \mu\text{m}^2$ in B6.ROP Os/+ mice) ($P < 0.001$) (Table 2) (Fig. 1). This increase in glomerular area resulted from an increase in cellularity (43 ± 2 cells/glomerular cross-section in control mice vs. 64 ± 4 cells/glomerular cross-section in B6.ROP Os/+ mice) ($P < 0.001$) and accumulation of extracellular matrix. The hypercellularity was the result of an increase in cell proliferation as assessed by PCNA stain ($P < 0.05$) (Table 2), as well as an influx of macrophages (1.2 ± 0.2 macrophages/glomerular cross-section in control mice vs. 3.6 ± 0.7 cells/glomerular cross-section in B6.ROP Os/+ mice) ($P < 0.01$). The silver-stained area of the glomerulus, representing extracellular matrix, increased from $179 \pm 15 \mu\text{m}^2$ in wild-type animals to $355 \pm 29 \mu\text{m}^2$ in B6.ROP Os/+ mice ($P < 0.01$) (Table 2) (Fig. 1). A similar increase was noted for collagen IV, an important component of ex-

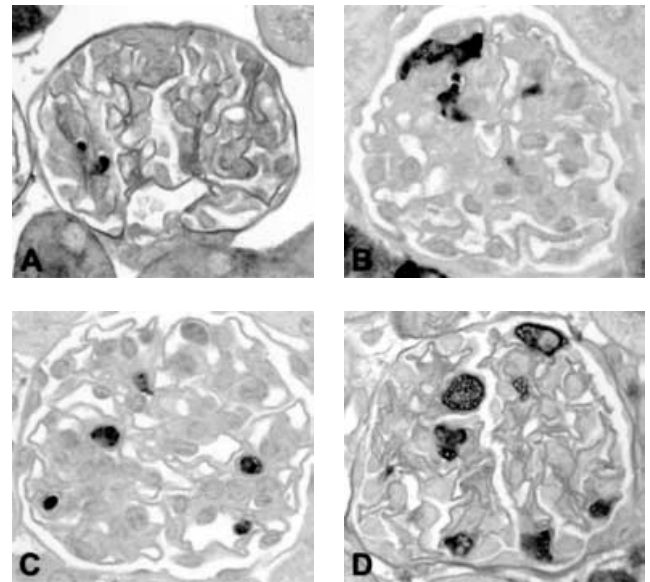


Fig. 2. Glomerular macrophage influx in control and hyperlipidemic mice. (A) Chow-fed C57BL/6 wild-type mice show only occasional glomerular macrophages. (B) Feeding of a high fat, high cholesterol diet to C57BL/6 mice does not increase glomerular macrophage influx but leads signs of lipid accumulation (foam cells). (C) Chow fed B6.ROP Os/+ animals show increased levels of glomerular macrophages. (D) B6.ROP Os/+, fed a high fat, high cholesterol diet show high levels of glomerular macrophages and foam cells.

tracellular matrix ($237 \pm 24 \mu\text{m}^2$ in C57BL/6 controls vs. $563 \pm 28 \mu\text{m}^2$) ($P < 0.001$). The α -SMA score, a measure for mesangial cell activation, was also elevated in B6.ROP Os/+ mice ($P < 0.001$) (Table 2) (Fig. 3). No significant staining for apolipoprotein B could be detected in the glomeruli or the tubulointerstitium of B6.ROP Os/+ mice.

The tubular parenchyma showed a modest degree of tubular dilation and atrophy. The tubulointerstitium demonstrated high number of macrophages ($P < 0.05$) (Table 2) (Fig. 2). Cellular turnover of tubular epithelial cells was not changed compared to control mice. No significant fibrosis was noted.

Hyperlipidemia led to a further decline in renal function in B6.ROP Os/+ mice

Feeding of the HFHC diet led to a significant increase in plasma cholesterol in B6.ROP Os/+ mice (361 ± 41 mg/dL with HFHC diet vs. 71 ± 3 mg/dL on regular chow) ($P < 0.001$) (Table 1). Triglyceride levels were decreased by the HFHC diet (36 ± 5 mg/dL on normal diet vs. 18 ± 3 mg/dL on the HFHC diet) ($P < 0.01$). Hyperlipidemic B6.ROP Os/+ mice had a further decline in renal function compared to normolipidemic B6.ROP Os/+ animals as expressed by an increase of plasma BUN from 45 ± 4 mg/dL on the chow diet to 62 ± 2 mg/dL on the HFHC diet ($P < 0.05$) but proteinuria remained unchanged to the elevated levels of normolipidemic B6.ROP Os/+.

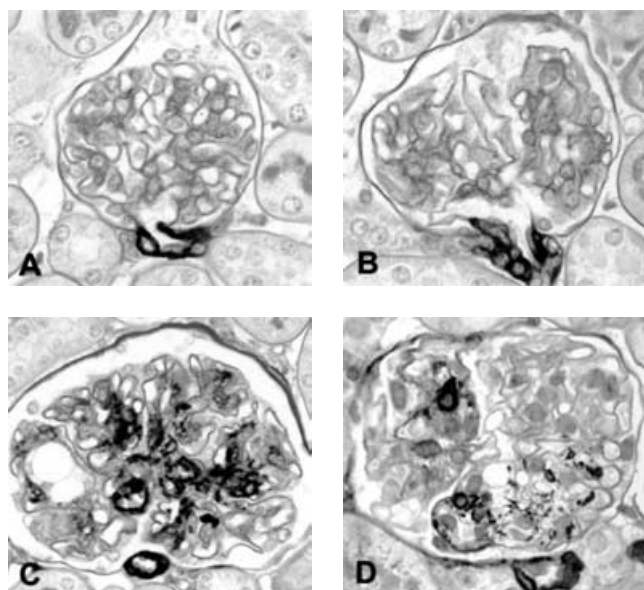


Fig. 3. Glomerular α -smooth muscle actin staining (α -SMA) in control and hyperlipidemic mice. Chow-fed C57BL/6 wild type mice (A) and C57BL/6 mice fed a high fat diet (B) did not show glomerular α -SMA staining and demonstrated positivity only in the arterioles. (C) Chow-fed B6.ROP Os/+ animals show a strong increase in mesangial positivity for α -SMA indicating activation of mesangial cells and changes toward a smooth muscle-like phenotype. (D) B6.ROP Os/+ mice fed a high fat, high cholesterol diet demonstrate strong positivity for α -SMA but decreased expression in areas of fat accumulation and mesangiolysis.

Hyperlipidemia aggravated renal pathology in B6.ROP Os/+ mice

Hyperlipidemic B6.ROP Os/+ mice had significant glomerular hypertrophy compared to wild type mice ($5414 \pm 159 \mu\text{m}^2$ vs. $3679 \pm 134 \mu\text{m}^2$ in C57BL/6 animals) ($P < 0.001$) but glomerular architecture was more altered than in normolipidemic B6.ROP Os/+ animals. Glomeruli frequently displayed signs of mesangiolysis; α -SMA expression, although still elevated compared to C57BL/6 control mice, was decreased in these areas (Table 2) (Fig. 3). Glomeruli commonly showed mesangial lipid deposits and diffuse or focal staining for apolipoprotein B (Fig. 5), mostly in the area of the vascular pole. Glomerular extracellular matrix increased from occupying $5.8 \pm 0.3\%$ to $7.1 \pm 0.3\%$ of the glomerular area in hyperlipidemic mice ($P < 0.05$) and glomerular collagen IV expression increased from $8.7 \pm 0.2\%$ to $12.2 \pm 0.4\%$ in animals fed the HFHC diet compared to normolipidemic B6.ROP Os/+ mice ($P < 0.05$). In addition, hypercellularity also increased in hyperlipidemic B6.ROP Os/+ mice compared to normolipidemic controls from a cellular area of $10.5 \pm 0.5\%$ of the glomerulus to $12.4 \pm 0.2\%$, respectively ($P < 0.01$) (Table 1). However, glomerular proliferation rate was unchanged and glomerular macrophage content was even slightly lower than in normolipidemic mice (2.0 ± 0.1 mac-2-positive cells/glomerular cross-section vs. 3.6 ± 0.7 mac-2-positive cells/glomerular cross-section in chow-

fed B6.ROP Os/+ mice) ($P < 0.05$) (Fig. 2) though macrophages were mostly foam cell-like in appearance and sometimes demonstrated staining for apolipoprotein B (Fig. 5).

Tubulointerstitial changes in hyperlipidemic B6.ROP Os/+ animals included fatty tubular degeneration in addition to the tubular atrophy and dilation seen in B6.ROP Os/+ mice on a regular diet. Tubular epithelial cells had a significantly increased cell turnover with PCNA staining cells being increased from 1.8 ± 0.2 /high power field in normolipidemic mice to 9.8 ± 1.4 positive cells/high power field in hyperlipidemic B6.ROP Os/+ animals ($P < 0.001$) (Fig. 4) and tubular TUNEL staining was also elevated although they did not reach the level of statistical significance (0.1 ± 0.0 TUNEL-positive cells/high power field in B6.ROP Os/+ mice vs. 0.6 ± 0.0 TUNEL-positive cells/high power field in B6.ROP Os/+ mice on the HFHC diet) ($P = 0.099$) (Fig. 4). Tubulointerstitial macrophage influx was elevated compared to C57BL/6 control mice and macrophages had mostly a foam cell-like phenotype (0.2 ± 0.0 in control animals vs. 3.7 ± 0.5 cells/high power field in hyperlipidemic B6.ROP Os/+ mice) ($P < 0.001$). The tubulointerstitium also showed infiltrating cells that stained positive for apolipoprotein B (Fig. 5).

Influences of the ROP Os/+ mutation on kidney function and renal pathology in hyperlipidemic mice

Reduction of renal mass by the ROP mutation led to an increase in plasma BUN in B6.ROP mice on the HFHC diet compared to wild-type mice on HFHC diet while proteinuria was not further increased (Table 1). Glomerular injury in hyperlipidemic B6.ROP mice seemed to be aggravated compared to wild-type mice on the HFHC diet as expressed by an increase in glomerular size and glomerular collagen IV accumulation (Table 2) (Fig. 1). In addition, glomerular α -SMA expression was increased in hyperlipidemic B6.ROP mice compared to hyperlipidemic wild-types (Fig. 3). The reduction in glomerular mass induced by the ROP Os/+ mutation seemed to have no influence on glomerular macrophages, proliferating cells, or apoptotic cells which were not different between both hyperlipidemic groups. Markers of tubulointerstitial changes like macrophage influx and tubuloepithelial cell turnover measured in proliferating and apoptotic cells were also not significantly different between these two groups.

Electron microscopy

Electron microscopy in a few selected cases showed an expansion of the mesangium in chow-fed B6.ROP Os/+ mice with an increase in actin filaments. Mesangial areas displayed frequent infiltration with macrophages. Hyperlipidemia led to the deposition of fat in the mesangial matrix and in the subendothelial areas of capillary

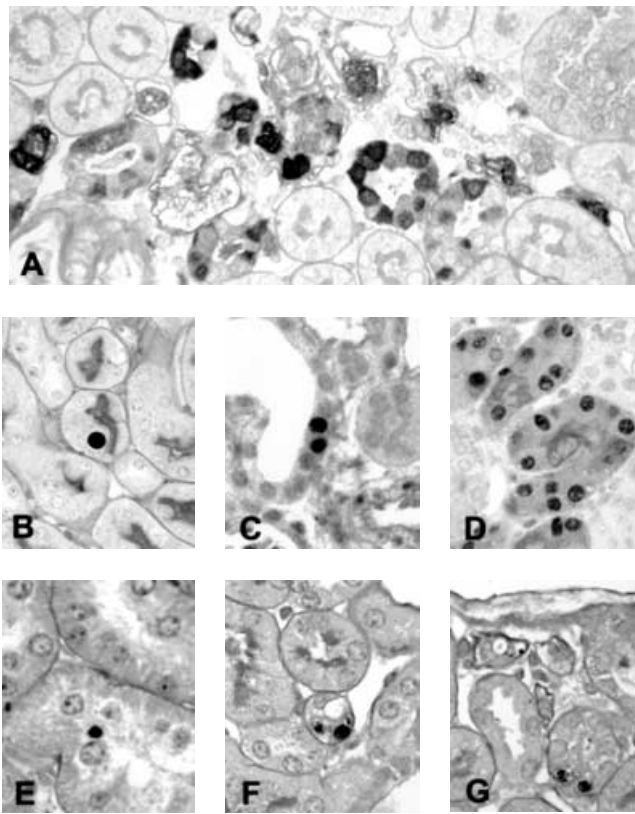


Fig. 4. Tubular changes in control and hyperlipidemic mice. (A) Low power view of the tubulointerstitium of a B6.ROP Os/+ mouse fed a high fat, high cholesterol diet stained for macrophages (Mac-2) and counterstained with periodic acid-Schiff (PAS)/methyl green. The photographs show prominent macrophage invasion in areas of tubular damage (arrow). (B, C, and D) Representative tubulointerstitial areas stained with the proliferation marker proliferating cell nuclear antigen (PCNA). (B) Only occasional cellular positivity in a wild-type mouse. (C) A B6.ROP Os/+ animal with typical tubular dilation (*) and associated proliferation of tubular epithelial cells. (D) B6.ROP Os/+ animal fed a high fat, high cholesterol diet with high levels of tubular epithelial cell proliferation in areas of tubular damage. (E, F, and G) Terminal deoxy transferase uridine triphosphate nick end labeling (TUNEL) staining for apoptotic cell death. Wild-type animals (E) show rare apoptotic cells while chow-fed B6.ROP Os/+ animals (F) and B6.ROP Os/+ mice fed a high fat, high cholesterol diet (G) showed increased apoptotic rates in areas of tubular damage.

walls as well as to the infiltration of the mesangium with macrophages with a foam cell appearance (Fig. 6).

Renal pathology was associated with changes in the expression levels of glomerular cytokines and chemokines

In situ hybridization was performed to assess whether changes in renal pathology were mediated by glomerular expression of different cytokines and chemokines. Glomerular expression of TGF- β mRNA was increased in hyperlipidemic C57BL/6 mice, B6.ROP Os/+ mice, and hyperlipidemic B6.ROP Os/+ animals (relative scores of 0.2 ± 0.1 in normal controls to 1.6 ± 0.2 , 1.3 ± 0.2 , and 1.4 ± 0.1 , respectively) ($P < 0.001$). The intraglomerular expression of TGF- β mRNA correlated with the amount of extracellular matrix assessed by black

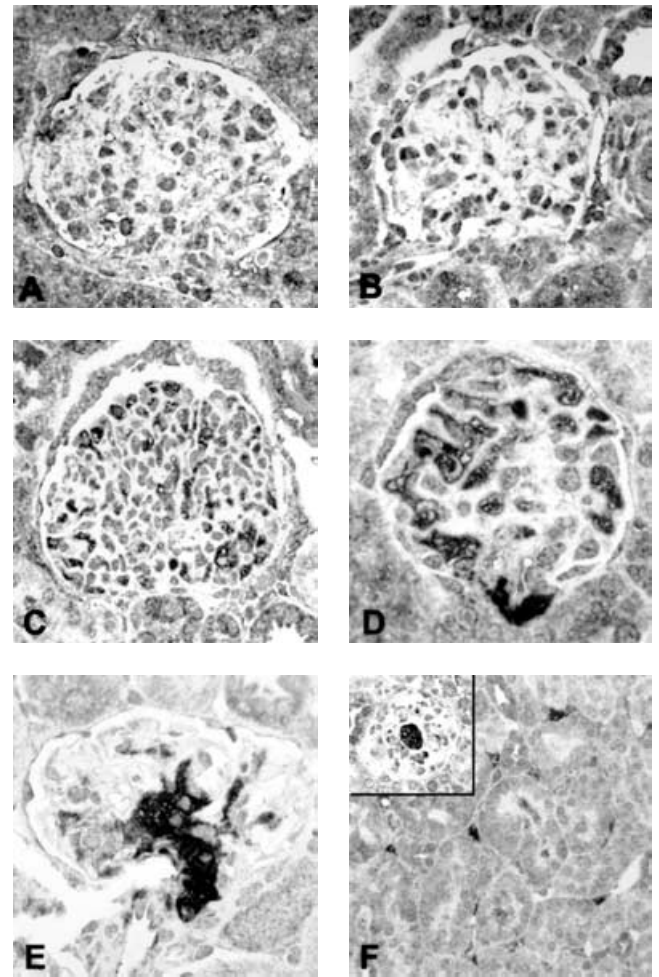


Fig. 5. Apolipoprotein B staining in control and hyperlipidemic mice. (A) Representative glomerulus from a chow-fed C57BL/6 mouse, no significant staining for apolipoprotein B. (B) Chow-fed B6.ROP Os/+, no significant staining for apolipoprotein B. (C) Glomeruli for C57BL/6 mice fed a high fat, high cholesterol diet show diffuse staining for apolipoprotein B. (D and E) Diffuse glomerular staining for apolipoprotein B with focal concentration in the area of the vascular pole in B6.ROP Os/+ animal fed a high fat, high cholesterol diet. (F) Apolipoprotein B staining in infiltrating tubulointerstitial cells and glomerular foam cell (insert) of tissue from a B6.ROP Os/+ animal fed a high fat, high cholesterol diet.

staining material in PAM stain ($r = 0.53$, $P < 0.01$) and with glomerular collagen IV content ($r = 0.59$, $P < 0.01$). It also showed a significant association with intraglomerular macrophage content ($r = 0.55$, $P < 0.01$), which has previously shown to be a contributor to total glomerular TGF- β expression [23, 24].

Similarly, hyperlipidemic control mice and ROP Os/+ mice showed a strong increase in glomerular PDGF-B mRNA expression and its receptor PDGF receptor β with a further increase in hyperlipidemic ROP Os/+ animals (Table 3). Both, PDGF-B and its receptor, correlated with glomerular cellularity ($r = 0.63$, $P < 0.01$ and $r = 0.5$, $P < 0.05$, respectively).

Renal expression of the chemoattractant MCP-1 was generally low with no positive cells in control mice and

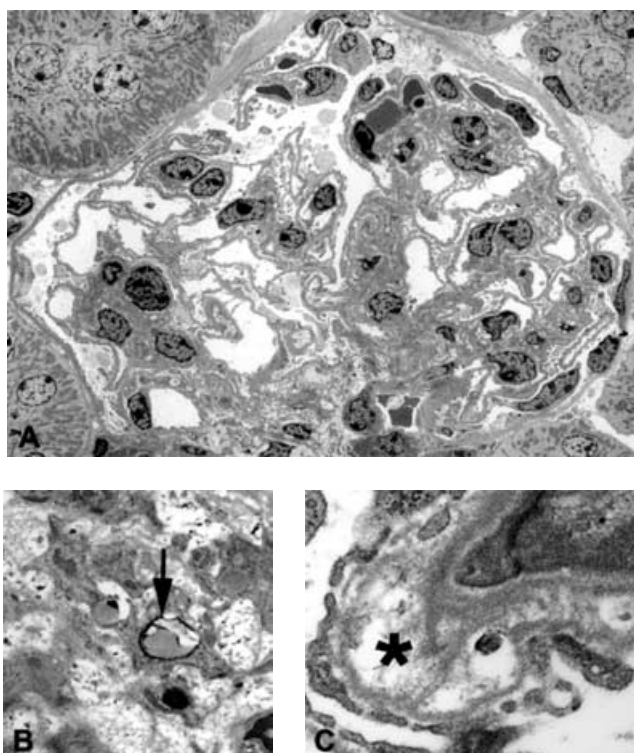


Fig. 6. Hyperlipidemic mice show ultrastructural alterations. (A) B6.ROP Os/+ mouse fed a high fat, high cholesterol diet. The mesangial area is expanded with an increase in dense bodies representing actin filaments and macrophage invasion. (B) B6.ROP Os/+ animal fed a high fat, high cholesterol diet. Electron microscopy reveals fat droplet in the mesangial area (arrow). (C) Expansion of the subendothelial area (*) in a B6.ROP Os/+ mouse on a high fat, high cholesterol diet.

Table 3. Glomerular cytokine mRNA expression

	C57BL/6, chow	C57BL/6+ high fat diet	B6.ROP Os/+ chow	B6.ROP Os/+ high fat diet
TGF- β 1	0.1 \pm 0.0	0.9 \pm 0.1 ^b	1.1 \pm 0.1 ^b	1.1 \pm 0.1 ^b
PDGF-B	0.2 \pm 0.1	1.8 \pm 0.1 ^a	1.7 \pm 0.2 ^a	2.4 \pm 0.1 ^{b,d,e}
PDGF receptor β	0.1 \pm 0.1	2.2 \pm 0.2 ^b	1.4 \pm 0.2 ^b	2.1 \pm 0.2 ^{b,c}

Abbreviations are: TGF- β 1, transforming growth factor- β 1; PDGF-B, platelet-derived growth factor-B.

Semiquantitative scoring of glomerular mRNA expression for TGF- β , PDGF-B and PDGF receptor β . Data expressed as mean \pm SEM. Statistical significances compared to wild-type controls (^a P < 0.01, ^b P < 0.001) or compared to chow fed B6.ROP Os/+ animals (^c P < 0.05, ^d P < 0.01). Differences between C57BL/6 mice and B6.ROP Os/+ mice on high fat diet are expressed as ^e P < 0.01.

only few positive cells in glomeruli, interstitial cells or cells of the vessel wall in the other experimental groups. Consequently, no statistical analysis was not performed for this parameter.

Hyperlipidemic mice do not develop obesity, hyperglycemia, and insulin resistance

To assess whether the deterioration in renal function and the aggravation of renal pathology was due to hyperlipidemia and not to changes mediated by obesity, hy-

perglycemia, or insulin resistance, body weight as well as glucose and insulin levels were assessed in mice from all experimental groups. Feeding a HFHC diet to C57BL/6 wild-type mice did not induce an increase in body weight and did not influence glucose metabolism as indicated by serum glucose and insulin levels (Table 1) as previously described [25]. Similarly, feeding this diet to B6.ROP Os/+ mice did not induce obesity (22.3 \pm 1.2 g body weight in chow fed B6.ROP Os/+ mice vs. 19.2 \pm 0.5 g in B6.ROP Os/+ mice on the HFHC diet) and there was no increase in glucose or insulin levels induced by feeding the HFHC diet (Table 1).

DISCUSSION

The capacity of hyperlipidemia to initiate or significantly contribute to chronic renal injury remains unsettled. In humans the role of hyperlipidemia in initiating kidney disease seems to be limited to some rare forms of metabolic abnormalities such as lecithin:cholesterol acyltransferase (LCAT) deficiency [26] and disorders of apolipoprotein E [27]. The extent to which hyperlipidemia might contribute to such chronic renal injury as diabetes or nephrosclerosis is not yet clear. The situation is different in experimental settings where hyperlipidemia has been demonstrated to induce renal injury in a variety of animal models such as dietary induced hyperlipidemia in rat [28–30], guinea pig [31], and rabbit [32], as well as in genetic hyperlipidemia in the obese Zucker rat [33] and the apolipoprotein E $-/-$ mouse [34]. In this study we examined the effect of hyperlipidemia in mice with reduced nephron mass, a situation common in humans as a result of aging, remote glomerulonephritis, vascular disease, or nephrectomy. We demonstrate that feeding a HFHC diet to C57BL/6 mice led to a decline in renal excretory function and to the development of proteinuria. These changes correlated with an increase in mesangial matrix and cellularity and by tubulointerstitial alterations including macrophage influx and an increased turnover of tubular epithelial cells. In addition, we could establish that hyperlipidemia aggravates renal injury in B6.ROP Os/+ mice. Hyperlipidemic B6.ROP Os/+ animals had an additional increase in plasma BUN levels and showed augmentation of ROP Os/+ associated renal pathology with the presence of mesangiolysis and a further increase in glomerular matrix and cellularity compared to normolipidemic B6.ROP Os/+ mice. Tubulointerstitial changes consisted of fatty tubular degeneration with an increase in the proliferation index of tubular epithelial cells and infiltration of macrophages/foam cells.

The mechanism by which hyperlipidemia exerts its deleterious effect on the kidney is still largely unknown. One mechanism by which hyperlipidemia may mediate renal injury could be by directly acting on resident cells in the kidney. The glomerulus and the renal

tubulointerstitium may be a preferred location for lipid deposition and interaction with resident cells because of the lack of a basement membrane separating the mesangium and the capillary stream and the presence of fenestrated epithelium lining glomerular and peritubular capillaries. Lipids can therefore easily access these areas and influence local metabolism. Mesangial cells have been shown to bind and take up native and oxidized low-density lipoprotein (LDL) cholesterol [35]. Binding of LDL and other lipoproteins to mesangial cells has been shown to influence cellular proliferation and stimulate secretion of inflammatory mediators like prostanoids, interleukin-6 (IL-6), PDGF, and TGF- β [35–38]. In addition, lipoproteins influence matrix generation by stimulating mesangial fibronectin and collagen IV expression [39, 40]. Consistent with this scenario, we were able to demonstrate that hyperlipidemic mice in our study had increased levels of glomerular expression of TGF- β , PDGF-B and its receptor PDGF receptor β . The relative expression of glomerular mRNA of these cytokines was significantly correlated with the amount of glomerular matrix and cellularity, respectively, making these growth factors likely contributors to the injury process. However, our results demonstrate only a correlation and not a definitive proof of causality.

Lipoproteins, the transport entities for lipids in the blood, may play a role in renal injury as well. Apolipoprotein B has been linked to the development of atherosclerosis and cardiovascular disease [41–43] and there have also been some studies that demonstrate an association of apolipoprotein B plasma levels and the progression of renal insufficiency [12, 44–46]. Normolipidemic control and B6.ROP Os/+ mice in our study did not show significant staining for apolipoprotein B in either glomeruli or the tubulointerstitium. In contrast, hyperlipidemic C57BL/6 animals demonstrated diffuse glomerular staining for apolipoprotein B and additional staining of interstitial cells that morphologically appeared to be infiltrating macrophages. In addition to this finding, the hyperlipidemic B6.ROP Os/+ mice had frequent, focal staining for apolipoprotein B in the area of the vascular pole that could not be seen in hyperlipidemic control animals. One explanation for this distinct staining pattern could be that these mice have impaired clearing of lipids through a mesangial pathway as an indicator of glomerular injury. However, our study does not address the issue whether trapping of apolipoprotein B in the glomeruli itself is able to induce renal damage or if this localization is incidental to the principal mechanism of tissue injury.

A mechanism that may be important in the mediation of lipid-induced renal injury involves infiltrating macrophages. Lipids have been shown to induce glomerular expression of chemoattractants such as MCP-1, monocyte-colony-stimulating factor (M-CSF), migration inhibitory factor (MIF), intercellular adhesion molecule-1 (ICAM-1), and vascular cell adhesion

molecule-1 (VCAM-1) [47–49] and various animal models of hyperlipidemia-induced renal disease have demonstrated increased influx of macrophages into glomeruli [28, 30, 34, 50] and into the tubulointerstitium [23, 29, 51, 52] of affected animals. The functional importance of macrophages in mediating renal injury in hyperlipidemic states is highlighted by work done by Pesek-Diamond et al [51] showing that depletion of macrophages resulted in an amelioration of renal function impairment and reduction of glomerulosclerosis and matrix expansion in hyperlipidemic rats with acute puromycin aminonucleoside nephrosis. Our studies tested this mechanism by directly assessing monocyte/macrophage infiltration and production of a major chemoattractant for these cells, MCP-1. Hyperlipidemic C57BL/6 mice in our study did not show significant expression of MCP-1 in either the glomeruli or the interstitium, corresponding to the low increase in glomerular macrophage content. However, hyperlipidemia did induce tubulointerstitial influx of macrophages/foam cells, presumably mediated by chemoattractants other than MCP-1. Studies have also indicated that macrophages from hyperlipidemic rats may be a major source for increased TGF- β expression [23, 24], an important cytokine for mediating extracellular matrix deposition [53]. Our study also demonstrated a significant correlation between glomerular macrophage content and TGF- β expression.

CONCLUSION

We have been able to show that hyperlipidemia leads to significant renal injury associated with a decline in renal function in healthy C57BL/6 control mice and that it is able to aggravate renal injury of reduced renal mass induced by the ROP Os/+ mutation. TGF- β and the PDGF-B system have been identified as two possible mediators of this process.

ACKNOWLEDGMENT

The authors would like to thank Xiangling Yang and Zandro Paredes for excellent technical assistance. This work was supported in part by a grant from the NIH (HL 52848).

Reprint requests to Charles E. Alpers, University of Washington Medical Center, Department of Pathology, Box 356100, 1959 NE Pacific Street, Seattle, WA 98195.
E-mail: calp@u.washington.edu

REFERENCES

1. MITCH WE, WALSER M, BUFFINGTON GA, et al: A simple method of estimating progression of chronic renal failure. *Lancet* 2:1326–1328, 1976
2. WILLIAMS PS, FASS G, BONE JM: Renal pathology and proteinuria determine progression in untreated mild/moderate chronic renal failure. *Q J Med* 67:343–354, 1988
3. NOVICK AC, GEPHARDT G, GUZ B, et al: Long-term follow-up after partial removal of a solitary kidney. *N Engl J Med* 325:1058–1062, 1991
4. SOLOMON LR, MALICK NP, LAWLER W: Progressive renal failure in a remnant kidney. *Br Med J (Clin Res Ed)* 291:1610–1611, 1985

5. PRAVTCHEVA DD, WISE TL: A postimplantation lethal mutation induced by transgene insertion on mouse chromosome 8. *Genomics* 30:529–544, 1995
6. PRAVTCHEVA DD, WISE TL: A transgene-induced mitotic arrest mutation in the mouse allelic with oligosyndactylism. *Genetics* 144:1747–1756, 1996
7. ZALUPS RK: The Os/+ mouse: A genetic animal model of reduced renal mass. *Am J Physiol* 264:F53–F60, 1993
8. HE C, ZALUPS RK, HENDERSON DA, et al: Molecular analysis of spontaneous glomerulosclerosis in Os/+ mice, a model with reduced nephron mass. *Am J Physiol* 269:F266–F273, 1995
9. ESPOSITO C, HE CJ, STRIKER GE, et al: Nature and severity of the glomerular response to nephron reduction is strain-dependent in mice. *Am J Pathol* 154:891–897, 1999
10. ZHENG F, STRIKER GE, ESPOSITO C, et al: Strain differences rather than hyperglycemia determine the severity of glomerulosclerosis in mice. *Kidney Int* 54:1999–2007, 1998
11. MASCHIO G, OLDRIZZI L, RUGIU C, et al: Serum lipids in patients with chronic renal failure on long-term, protein-restricted diets. *Am J Med* 87:51N–54N, 1989
12. SAMUELSSON O, AURELL M, KNIGHT-GIBSON C, et al: Apolipoprotein-B-containing lipoproteins and the progression of renal insufficiency. *Nephron* 63:279–285, 1993
13. SASAKI T, KURATA H, NOMURA K, et al: Amelioration of proteinuria with pravastatin in hypercholesterolemic patients with diabetes mellitus. *Jpn J Med* 29:156–163, 1990
14. SHOJI T, NISHIZAWA Y, TOYOKAWA A, et al: Decreased albuminuria by pravastatin in hyperlipidemic diabetics. *Nephron* 59:664–665, 1991
15. RABELINK AJ, HENE RJ, ERKELENS DW, et al: Partial remission of nephrotic syndrome in patient on long-term simvastatin. *Lancet* 335:1045–1046, 1990
16. SEGERER S, HUDKINS KL, TANEDA S, et al: Oral interferon-alpha treatment of mice with cryoglobulinemic glomerulonephritis. *Am J Kidney Dis* 39:876–888, 2002
17. HUGO C, SHANKLAND SJ, BOWEN-POPE DF, et al: Extraglomerular origin of the mesangial cell after injury. A new role of the juxtaglomerular apparatus. *J Clin Invest* 100:786–794, 1997
18. HIROMURA K, HASELEY LA, ZHANG P, et al: Podocyte expression of the CDK-inhibitor p57 during development and disease. *Kidney Int* 60:2235–2246, 2001
19. SEGERER S, EITNER F, CUI Y, et al: Cellular injury associated with renal thrombotic microangiopathy in human immunodeficiency virus-infected macaques. *J Am Soc Nephrol* 13:370–378, 2002
20. TANEDA S, HUDKINS KL, CUI Y, et al: Growth factor expression in a murine model of cryoglobulinemia. *Kidney Int* 63:576–590, 2003
21. ALPERS CE, HUDKINS KL, PRITZL P, et al: Mechanisms of clearance of immune complexes from peritubular capillaries in the rat. *Am J Pathol* 139:855–867, 1991
22. ALPERS CE, HUDKINS KL, GOWN AM, et al: Enhanced expression of “muscle-specific” actin in glomerulonephritis. *Kidney Int* 41:1134–1142, 1992
23. DING G, PESEK-DIAMOND I, DIAMOND JR: Cholesterol, macrophages, and gene expression of TGF-beta 1 and fibronectin during nephrosis. *Am J Physiol* 264:F577–F584, 1993
24. DING G, VAN GOOR H, FRYE J, et al: Transforming growth factor-beta expression in macrophages during hypercholesterolemic states. *Am J Physiol* 267:F937–F943, 1994
25. SCHREYER SA, WILSON DL, LEBOEUF RC: C57BL/6 mice fed high fat diets as models for diabetes-accelerated atherosclerosis. *Atherosclerosis* 136:17–24, 1998
26. JIMI S, UESUGI N, SAKU K, et al: Possible induction of renal dysfunction in patients with lecithin:cholesterol acyltransferase deficiency by oxidized phosphatidylcholine in glomeruli. *Arterioscler Thromb Vasc Biol* 19:794–801, 1999
27. WATANABE Y, OZAKI I, YOSHIDA F, et al: A case of nephrotic syndrome with glomerular lipoprotein deposition with capillary ballooning and mesangiolysis. *Nephron* 51:265–270, 1989
28. KASISKE BL, O'DONNELL MP, SCHMITZ PG, et al: Renal injury of diet-induced hypercholesterolemia in rats. *Kidney Int* 37:880–891, 1990
29. JOLIS JA, KUNTER U, JANSSEN U, et al: Early mechanisms of renal injury in hypercholesterolemic or hypertriglyceridemic rats. *J Am Soc Nephrol* 11:669–683, 2000
30. GUIJARRO C, KASISKE BL, KIM Y, et al: Early glomerular changes in rats with dietary-induced hypercholesterolemia. *Am J Kidney Dis* 26:152–161, 1995
31. AL-SHEBEB T, FROHLICH J, MAGIL AB: Glomerular disease in hypercholesterolemic guinea pigs: A pathogenetic study. *Kidney Int* 33:498–507, 1988
32. YOSHIMURA N, ARIMA S, NAKAYAMA M, et al: Renal impairment and intraglomerular mononuclear phagocytes in cholesterol-fed rabbits. *Nephron* 68:473–480, 1994
33. KAMANNA VS, KIRSCHENBAUM MA: Association between very-low-density lipoprotein and glomerular injury in obese Zucker rats. *Am J Nephrol* 13:53–58, 1993
34. WEN M, SEGERER S, DANTAS M, et al: Renal injury in apolipoprotein e-deficient mice. *Lab Invest* 82:999–1006, 2002
35. CORHITSIDIS G, RIFICI V, GUPTA S, et al: Preferential binding of oxidized LDL to rat glomeruli in vivo and cultured mesangial cells in vitro. *Kidney Int* 39:858–866, 1991
36. WASSERMAN J, SANTIAGO A, RIFICI V, et al: Interactions of low density lipoprotein with rat mesangial cells. *Kidney Int* 35:1168–1174, 1989
37. WHEELER DC, CHANA RS, TOPLEY N, et al: Oxidation of low density lipoprotein by mesangial cells may promote glomerular injury. *Kidney Int* 45:1628–1636, 1994
38. NISHIDA Y, ODA H, YORIOKA N: Effect of lipoproteins on mesangial cell proliferation. *Kidney Int* 56(Suppl 71):S51–S53, 1999
39. ROVIN BH, TAN LC: LDL stimulates mesangial fibronectin production and chemoattractant expression. *Kidney Int* 43:218–225, 1993
40. KIM SB, KANG SA, CHO YJ, et al: Effects of low density lipoprotein on type IV collagen production by cultured rat mesangial cells. *Nephron* 67:327–333, 1994
41. LAMARCHE B, DESPRES JP, MOORJANI S, et al: Prevalence of dyslipidemic phenotypes in ischemic heart disease (prospective results from the Quebec Cardiovascular Study). *Am J Cardiol* 75:1189–1195, 1995
42. GRUNDY SM: Low-density lipoprotein, non-high-density lipoprotein, and apolipoprotein B as targets of lipid-lowering therapy. *Circulation* 106:2526–2529, 2002
43. PURCELL-HUYNH DA, FARESE RV, JR., JOHNSON DF, et al: Transgenic mice expressing high levels of human apolipoprotein B develop severe atherosclerotic lesions in response to a high-fat diet. *J Clin Invest* 95:2246–2257, 1995
44. ATTMAN PO, ALAUPOVIC P, SAMUELSSON O: Lipoprotein abnormalities as a risk factor for progressive nondiabetic renal disease. *Kidney Int* 56(Suppl 71):S14–S17, 1999
45. SAMUELSSON O, MULEC H, KNIGHT-GIBSON C, et al: Lipoprotein abnormalities are associated with increased rate of progression of human chronic renal insufficiency. *Nephrol Dial Transplant* 12:1908–1915, 1997
46. SAMUELSSON O, ATTMAN PO, KNIGHT-GIBSON C, et al: Complex apolipoprotein B-containing lipoprotein particles are associated with a higher rate of progression of human chronic renal insufficiency. *J Am Soc Nephrol* 9:1482–1488, 1998
47. HATTORI M, NIKOLIC-PATERSON DJ, MIYAZAKI K, et al: Mechanisms of glomerular macrophage infiltration in lipid-induced renal injury. *Kidney Int* 56(Suppl 71):S47–S50, 1999
48. KODAMA N, OTANI H, YAMADA Y, et al: Involvement of MCP-1 and M-CSF in glomerular foam cell formation in ExHC rats. *Kidney Int* 56(Suppl 71):S174–S177, 1999
49. MIYAZAKI K, ISBEL NM, LAN HY, et al: Up-regulation of macrophage colony-stimulating factor (M-CSF) and migration inhibitory factor (MIF) expression and monocyte recruitment during lipid-induced glomerular injury in the exogenous hypercholesterolaemic (ExHC) rat. *Clin Exp Immunol* 108:318–323, 1997
50. LAVAUD S, MICHEL O, SASSY-PRIGENT C, et al: Early influx of glomerular macrophages precedes glomerulosclerosis in the obese Zucker rat model. *J Am Soc Nephrol* 7:2604–2615, 1996
51. PESEK-DIAMOND I, DING G, FRYE J, et al: Macrophages mediate adverse effects of cholesterol feeding in experimental nephrosis. *Am J Physiol* 263:F776–F783, 1992
52. MATSUDA S, ARAI T, IWATA K, et al: A high-fat diet aggravates tubulointerstitial but not glomerular lesions in obese Zucker rats. *Kidney Int* 56(Suppl 71):S150–S152, 1999
53. SHANKLAND SJ, JOHNSON RJ: TGF-beta in glomerular disease. *Miner Electrolyte Metab* 24:168–173, 1998